High-fidelity Large Eddy Simulations of the Flame Transfer Function of a turbulent swirling spray flame.

A. Badhe*, D. Laera, L. Gicquel

CERFACS, 42 avenue Gaspard Coriolis, 31057 Toulouse, France

Abstract

This study addresses the use of high-fidelity Euler-Lagrange (EL) LES of turbulent spray flames subject to harmonic acoustic forcing in an attempt to predict the flame response, i.e. the so-called Flame-Transfer-Function (FTF). To do so, the SICCA-spray burner from the EM2C laboratory (CNRS, CentraleSupelec, Paris) is specifically addressed. In this first investigative step, the gain and phase (or characteristic time-delay) of the FTF are found to be sensitive to the fuel injection angle. Multiple simulations carried out with different injection angles (35 to 60 degrees) reveal a peculiar trend of the FTF gain and phase. For an increasing spray injection angle, the gain shows a decreasing bias while the phase (or time-delay) exhibits an increasing trend. Furthermore, the gain at the lowest angle (35 degrees) while the phase at the highest angle (60 degrees) are found to be in fair agreement with experimental values. Preliminary analyses performed using Dynamic-Mode-Decomposition (DMD) allows to explain such dynamics by identifying the regions of the flame / spray that activate in the different conditions.

Keywords:
Thermoacoustic instabilities, Flame Transfer Function (FTF), Turbulent spray flames, Euler-Lagrangian LES,, Acoustic Forcing.

1. Introduction

Thermoacoustic (TA) combustion instability is a recurring issue in gas turbine engines and has been a topic of intense research for many decades [1, 2]. Over the past years, Large-Eddy-Simulation (LES) as a simulation tool has been successfully utilized to predict such instabilities [3, 4] and has become an integral part of the design and development process in industry. However, the literature on the LES of combustion dynamics in liquid-fueled combustors [5–10] has started to appear only in recent years. Indeed, modeling of the liquid-phase physical processes such as primary, secondary, edge atomization, evaporation, liquid-wall interaction, multi-regime combustion in two-phase flames is still a great challenge in general and a topic of active research [11]. Two approaches exist for resolving the liquid-phase: the Eulerian-Eulerian (EE) formulation [12], or by tracking droplet trajectories as done in the Lagrangian approach [13] (EL).

When it comes to TA predictions by LES, one method is the brute force approach where the system is fully simulated to see if a so-called *self-excited regime* appears. In such an approach, the burner, if unstable, indeed resonates exhibiting instabilities with pressure oscillations increasing in amplitude until they reach a stable limit-cycle for given operating conditions and acoustic boundary conditions. Another commonly adopted method for investigating possible instabilities is to separate the complex flame dynamics from the combustor acoustics [14]. Reduced-ordered acoustic tools, such as Helmholtz solvers [15], network-models [16–18] are then employed for a more comprehensive system-level stability analysis. A crucial component of such investigations is the flame response model that describes the coupling between the unsteady heat-release and the acoustics, also known as the Flame-Transfer or Describing Functions (FTF/FDFs) usually expressed in the frequency domain [14, 15, 19]. In that case, FTF/FDFs are determined either from analytical expressions, experiments or LES where acoustic excitation of the flame in a controlled stable environment allows to measure the heat release oscillations [19, 20] for different frequencies and perturbation amplitudes. The present work particularly addresses this FTF prediction for turbulent swirling spray flames by employing the forced Euler-Lagrange LES approach. The objective is to qualify this method while assessing the uncertainties and sensitivity to the two-phase spray combustion models. Indeed, most gas turbine combustors employ pressure-swirled atomizers that inject liquid fuel as a swirling hollow cone spray. However, due to a lack of optical access inside the injection system, direct measurements of the spray angle or its fine characterisation are usually not possible. In reality, this spray injection angle is prone to some uncertainties due to its sensitivity to operating conditions such as fuel line pressure drop, to physical properties of the fuel [21, 22] and, as recently observed in the SICCA-spray combustor from EM2C laboratory (CNRS, CentraleSupelec, Paris) [23], also to the interaction of the liquid spray with the surrounding strong swirling flow [23–25].

Previously observed sensitivities have recently been confirmed at CERFACS while conducting LES of the self-excited thermoacoustic instability for this SICCA configuration. In-

*Corresponding author: badhe@cerfacs.fr

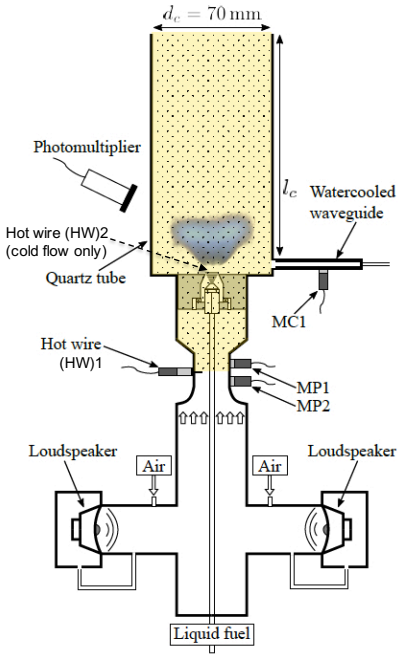

Figure 1: A schematic of the SICCA-spray combustor [26] with the portion considered for the LES highlighted in yellow. Image reproduced from [9]

deed, brute force predictions revealed that the coupling mechanism between the acoustic mode and the liquid film forming on the conical injector walls is fundamental to trigger and sustain the thermoacoustic limit cycle [7, 10]. Likewise, the impact of spray injection angle on the stability of the combustor was highlighted in [9]. Complementing these recently published results, the current work aims at investigating these issues of injection angle on the flame-acoustic-spray coupling under forced conditions over a range of frequencies in an attempt to characterize numerically the FTF.

2. Experimental FDF Measurements

The SICCA-Spray burner, shown in Fig. 1, comprises a plenum connected to a simple cylindrical flame tube through a swirl injection system containing a simplex pressure-swirled atomizer [10, 26]. Experimentally, the length of the tube can be changed to obtain thermoacoustically stable/unstable conditions. For example, in the previous work of Lo Schiavo et al. [7, 10], a longer tube of length $l_c = 280mm$ (see Fig. 1) was used wherein a self-sustained instability coupled with a quarter-wave longitudinal acoustic mode of the chamber was obtained. In the present context of forced spray flame, a stable setup is selected with a shorter flame tube of length $l_c = 165mm$. The burner is operated at a power rating of $\approx$ 6.4kW with 2.58g/s of air mass flow rate and 0.144 g/s of fuel resulting in a global equivalence ratio of 0.85 [10, 26]. To obtain the FTF/FDF, the experimental system is acoustically excited by means of two loudspeaker driving units mounted in the plenum [26, 27]. In this case and for FDF measurements, the driver units are operated at six different voltage levels $V_{0,pp}$ (500 mV to 1300 mV in steps of 200 mV) and a linear frequency sweep is performed from 300 Hz to 800 Hz, at each level. It is important to note that for a given voltage across the driver loudspeakers, the hot wire probe (HW1) in Fig. 1 measures different velocity fluctuations $u'/\bar{u}$ levels for different forcing frequencies [26]. Original measurements [26] were obtained with respect to the velocity perturbations at HW1, thus representing the *Injector+Flame* describing function ($\mathcal{F}_{IF}$) that included the dynamic acoustic response of the swirl injector. As a part of a recent effort at EM2C [27], the flame response of the flame ($\mathcal{F}_F$) was isolated from the swirl injector response ($\mathcal{F}_I$). This was achieved by characterizing the burner transfer function ($\mathcal{F}_I$) under cold flow conditions and by correlating the acoustic velocity fluctuations measured at a new location (HW2) near the flame root just above the injector lip and compared to measurements obtained at HW1. Doing so the injector+flame describing function could be reworked and rescaled to obtain the flame only transfer function. Note that the HW2 hot wire location (not shown in Fig. 1) is 2.5 mm above the backplane and 3 mm away from the central axis. Figure 2 provides the new gain and phase of the scaled describing function $\mathcal{F}_F$ as a function of the excitation frequency and voltages. The exercise of characterizing ($\mathcal{F}_F$) is also supported by the conclusions of Truffin and Poinsot [28] who recommended using a reference location close to the flame in such system response identification (irrespective of the method: *i.e.* in experiments or LES).

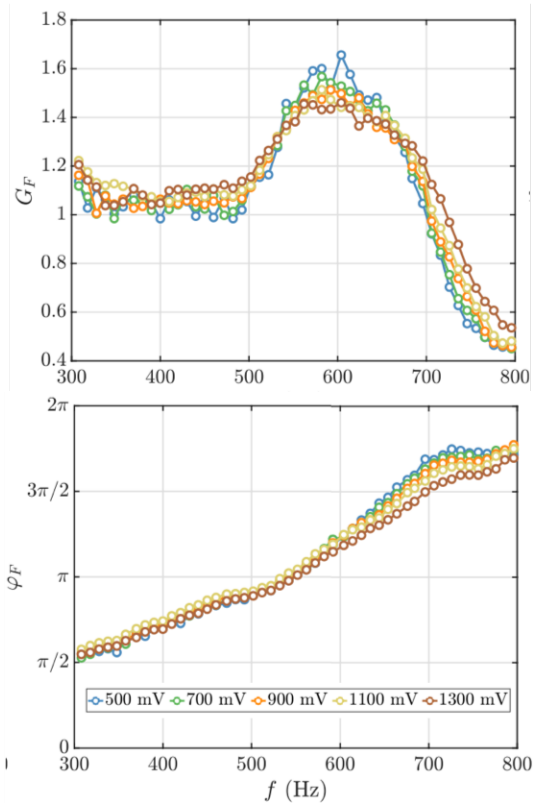

Figure 2: The experimental gain and phase plots of the FDF defined with respect to the velocity fluctuations at the flame root for different driver unit voltages: data form the work [23, 26, 27].

Note that a FDF, $\mathcal{F}_F$, provides the nonlinear response of the

flame to the incoming acoustic velocity perturbation and is defined as:

$$\mathcal{F}_F\left(\omega,\left|u_2'\right|\right)=\frac{\dot{Q}'\left(\omega,\left|u_2'\right|\right)/\overline{\dot{Q}}}{u_2'/\bar{u}_2}=G_F\left(\omega,\left|u_2'\right|\right)e^{i\varphi_F(\omega,|u_2'|)},\quad(1)$$

where, $u_2'/\bar{u}_2$ is acoustic velocity fluctuation levels at the flame root (HW2), and $G=|\mathcal{F}_F|$as well as $\varphi_F=arg(\mathcal{F}_F)$ are respectively the gain and phase of $\mathcal{F}_F$.

3. Numerical Setup

The LES computational domain retained for the present work is highlighted in yellow in Fig. 1. When it comes to the modelling or numerical strategies, these are briefly recalled since they are almost identical to our previous studies on the self-sustained instability. As for a detailed description and validation of the numerical approach, these can be found in Ref. [7]. The domain is discretized by approximately 20 M tetrahedral elements designed with a refinement of $\Delta x\simeq 150\,\mu$m in the finest region positioned at the flame root while $\Delta x\simeq 200-300\,\mu$m is used further downstream. For the simulations, the code AVBP developed by CERFACS (http://www.cerfacs.fr/avbp7x) solving the LES-filtered compressible Navier-Stokes equations is employed making use of the WALE model [29] for the turbulent closure. Flow integration is achieved using the the second-order in space and time Lax-Wendroff scheme. The inflow air mass flow rate is prescribed with a turbulent mean profile while ambient pressure is imposed at outlet boundary condition with the Navier-Stokes Characteristic Boundary Condition (NSCBC) treatments [30]. The flame in the following is then forced either from the inlet (as in the experiments) or from the outlet. In both cases, the acoustic boundary conditions at the inlet (and outlet) were almost non-reflecting [31, 32] so that all outgoing waves leave and no unphysical resonance establishes. The inlet velocity (or outlet pressure) is everytime excited at a specific frequency and the amplitude is adjusted to reach the desired velocity fluctuation level at HW2. Adiabatic non-slip walls are applied elsewhere aside from the quartz tube and chamber backplane where heat losses are taken into account through a heat resistance making use of the temperature value matching of the experiment. Chemical reaction is described by a global two-step six-species scheme $2S\_C7H16\_DP$ with Pre-Exponential Adjustment (PEA) [11]. Turbulent combustion is modelled using the two-phase flame extension of the dynamic thickened flame model (TP-TFLES) [11]. Note that spray flames are usually characterised by both premix and diffusion combustion regimes [7], so in order to guarantee a proper application of the thickened flame model, which is correctly defined only for premixed flames, an additional conditioning is applied using the Takeno flame index (FI) [33] classically defined as a function of the gradient of fuel and oxidizer mass fractions: $FI=\nabla Y_{C_7H_{16}}\cdot\nabla Y_{O_2}/|\nabla Y_{C_7H_{16}}\cdot\nabla Y_{O_2}|$.

As said previously, the liquid phase is modeled using a Lagrangian approach. The Schiller-Naumann correlation and the Abramzon and Sirignano model [34] describe drag and evaporation, respectively. Droplets are injected through a flat annulus positioned at the atomizer location using the FIMUR model [35]. It treats the injection of a hollow cone spray resulting from a simplex atomizer in which the axial and tangential components of injected liquid droplet velocity are formulated as a function of the fuel mass flow rate $\dot{m}_\ell$ and injection half-cone spray angle θ for a given atomizer orifice diameter D_0. $D_0=120\mu m$ is the value specified in current simulations. The FIMUR injection model also requires a droplet size distribution as input which is specified via a *Rosin-Rammler* probability density function (PDF) fitted from experimental measurements of mean (D_{10}) and Sauter diameters (SMD or D_{32}) taken at $z=2.5$ mm in the combustion chamber: $D_{10}=10\,\mu$m and $D_{32}=18\,\mu$m. As a consequence of the above adopted modelling strategy, any change in droplet diameter is only due to evaporation, neglecting phenomena like primary and secondary atomizations as well as splash and liquid film break-up at the edge of the conical injector wall.

Finally, for the liquid-wall interaction, the so-called FILM Lagrangian BC [7] is utilized in all computations. The film height and its speed are with this approach governed by the Saint-Venant equations [36] until the particles are released in the chamber at the injector lip. Note that, the FILM treatment for the liquid-wall interaction was found critical in triggering and retrieving the thermoacoustic limit-cycle oscillation in the self-excited LES [7].

4. Results and Discussion

In the following sections the global results of the LES predictions are presented. To evaluate the result sensitivity to the spray angle, three different cases characterised by different injection spray angles (θ) are individually performed: *i.e.* $\theta=35°$, $\theta=45°$ and $\theta=60°$. First, a brief qualitative validation of the Euler-Lagrange LES approach is provided by simulating a stable steady state flame before going on with the forced computations. Figure 3 (a) & (b) show the mean heat release rate (HR) from LES, (b), for the injection angle $\theta=45°$, and (a)

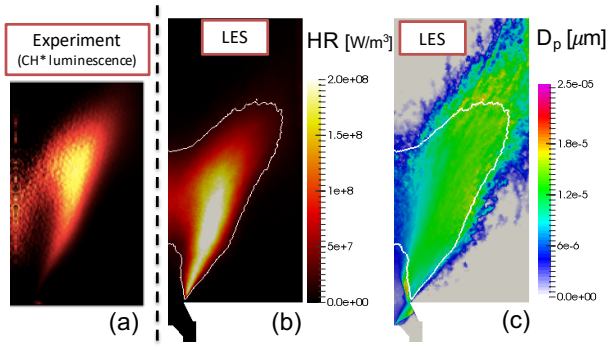

Figure 3: (a) Experiment: mean CH* chemiluminescence [26], (b) LES mean heat release rate distribution in the combustion chamber and (c) Mean fuel droplet diameter distribution in the combustion chamber, under stable steady operation. Spray injection angle is $\theta=45°$. White line is the iso-contour $\dot{q}=20MW/m^3$, $\sim 10\%$ of the max heat release, denoting the mean flame shape.

the flame shape observed experimentally. Good agreement with CH* chemiluminescence images [26] is confirmed here. As a complement, Fig. 3 (c) depicts the mean fuel droplet diameter distribution in the combustion chamber. Note that no significant differences are obtained at other injection angles for stable steady conditions (not shown here) and a systematic analysis can be be found in [9].

4.1. Inlet vs Outlet Forcing

For the calculation of the flame response, both inlet and outlet pulsing were explored and the equivalence of these two approaches is touched upon hereafter. In this specific work, the analysis is carried out only for one single operating point, *i.e.* low-amplitude forcing targeting the 500 mV case at **530 Hz**. This condition coincides with the frequency of the self-sustained limit-cycle observed in the unstable configuration ($l_c = 280mm$) during experiments [26] which was also analysed by the previous numerical works [7, 9, 10]. In the experiments when the stable configuration ($l_c = 165mm$) is forced [26] at this operating point, the velocity fluctuation levels recorded in plenum by HW1 $u'_{1,rms}/\bar{u}_1 = 0.40$ while at HW2 (above injector lip, and under cold flow conditions) these are $u'_{2,rms}/\bar{u}_2 = 0.13$. In both cases obtained flame responses, *i.e.* the gain and phase of $\mathcal{F}_I$, are provided in Table. (1) confirming the adequacy of both forcing conditions as well as obtained deviations in comparison to experimental findings.

The first line of Table.1 lists the FTF gain and time-delay (along with the phase) obtained from LES by pulsing the system from inlet boundary condition. It can be noted, if the inlet velocity amplitude is tuned to reach the desired velocity fluctuation level at the the flame root (HW2): $u'_{2,rms}/\bar{u}_2 = 0.13$, the resulting fluctuating velocity measured prior to the swirler at HW1 is $u'_{1,rms}/\bar{u}_1 = 0.54$ when it is experimentally measured at 0.4. This reveals a probable non perfect representation by the computational model of the acoustic properties of the plenum and injector domains. The impedance at the inlet boundary is indeed imprecise and considering the fact that this part of the rig is not modeled, the acoustic environment of LES might not be fully identical to the experiment. This result may also indicates that the discretization level chosen for the swirler vanes is not sufficient to correctly capture the impedance (or admittance) of the swirl injector. It should however be stressed that these inaccuracies did not influence the prediction of self-sustained limit-cycle in [7, 9, 10], the thermoacoustic oscillations being coupled with the first combustion chamber acoustic mode which is weakly influenced by the plenum acoustics (as discussed in Ref. [7]).

For the second line, results are provided for the pulsed simulation from the outlet boundary condition. Similarly to the inlet-forcing case, the outlet pressure oscillation level is tuned in order to achieve the desired fluctuation levels at HW2. If comparing the FTF obtained from thes two simulations, it is possible to conclude that the two forcing strategies reasonably match. This result is in line with what was shown by Gaudron *et. al.* [37], who experimentally investigated inlet and outlet forcing in the case of a turbulent swirling gaseous flame. Finally, comparing the two LES predictions with the experimental

Table 1: FTF's obtained by forcing LES from the inlet and the outlet along with available experimental data.

	Ref. HW1 $u'/\bar{u}$ **(rms)**	**Ref. HW2** $u'/\bar{u}$ **(rms)**	**Gain [-]**	**Delay [ms]**	**Phase [rad]**
LES $\mathcal{F}_F$ (inlet)	0.54	0.13	0.98	0.64	0.68π
LES $\mathcal{F}_F$ (outlet)	-	0.13	1.03	0.69	0.70π
EXP $\mathcal{F}_F$	0.40	0.13	1.27	0.90	0.96π

data (third line in Table 1), a mismatch of 20% in gain and 25% in phase is observed. To further examine the sensitivity of the flame response to the injection angle prescribed in the FIMUR model more simulations are conducted and detailed hereafter.

4.2. Impact of the Spray Injection Angle

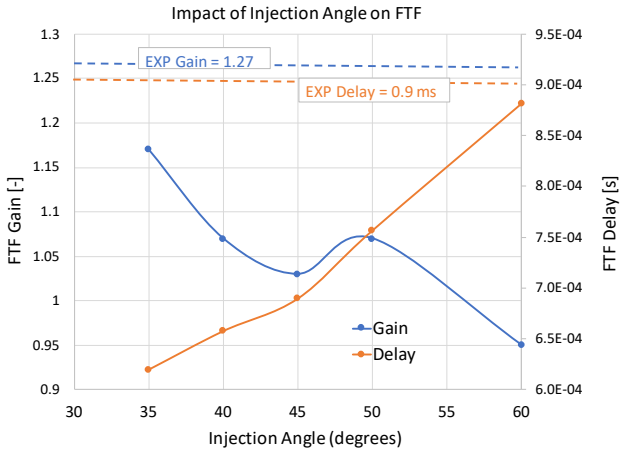

Figure 4: Opposing trend of the global Gain and Delay with injection angle.

The following analysis derives from the previous work of Lo Schiavo *et. al.* [9] where the impact of the spray injection angle on the self-sustained LES limit cycle predictions is investigated. To do so the outlet-forcing FTF computations at 530 Hz are proposed considering three different spray injection angles: $\theta = 35°$, $45°$ and $60°$.

Gain and phase variation as a function of θ are shown in Fig. 4. The $\theta = 45°$ case has been discussed in the previous section and is taken as reference in the discussion. Starting from this result, when reducing or increasing the spray angle, opposite trends are observed for the gain and the phase. At $\theta = 35°$, the FTF gain is reasonably close to the experimental value while the agreement between the global time-delay (or phase) is the worst. The opposite appears for $\theta = 60°$ although an almost perfect match is achieved for the FTF phase, the discrepancy in the gain increases. Note that the highlighted trend is similar at another operating point: *i.e.* forcing at 640 Hz (not discussed further in this article).

To further analyze these results, the LES data are post-processed using three dimensional Dynamic Mode Decomposition (DMD) [38] to reconstruct the dynamics of the system at the forcing frequency. The analysis is performed using about 280 snapshots for ≈ 30 cycles and considering the whole set of variables of interest for both the gaseous and the liquid phases: *i.e.* pressure, velocity, heat release rate, mass transfer rate and

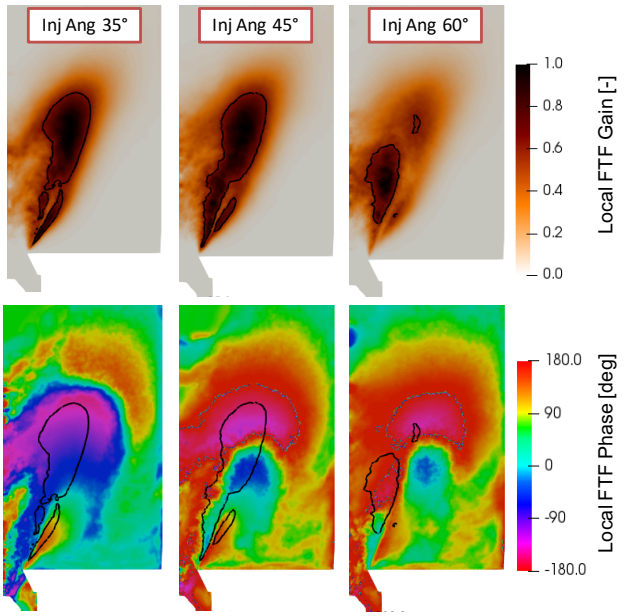

Figure 5: Local FTF Gain and Phase-delay obtained from 3D DMD and its variation with spray injection angle. Local FTF gain is normalized by its max value. Black contour line is the 60% of max value thus enclosing region of most intense heat release fluctuations.

liquid volume fraction... This allows to provide insight into the coherent oscillatory patterns both in the gas and the liquid phases while helping to distinguish variations in the local flame response for the different injection angles. Figure 5 shows the local field of the modulus (or magnitude) of the retrieved heat-release-rate (HR) fluctuations as well as its phase. Considerable differences in the oscillating HR patterns are observed due to the variations of the specified injection angle θ. Using these heat release DMD modes, a local FTF view is obtained by correlating the HR with the axial velocity perturbation at HW2 following:

$$Local\_FTF(\omega, \vec{x}) = \frac{\hat{q}(\omega, \vec{x})/\bar{q}(\vec{x})}{\hat{u}(\omega, x_{ref})/\bar{u}(x_{ref})} \quad (2)$$

where $\hat{(\cdot)}$ and $\bar{(\cdot)}$ denote the complex valued DMD variables (mode shape) and its mean respectively.

Thanks to this vision, a possible link with the trends shown in Fig. 5 and the different fuel droplet dynamics is now discussed. In general, the Lagrangian droplets impinging on the conical injector wall lose their initial momentum due to the film treatment [36]. Droplets are then released at a slower speed into the chamber. As already shown by Lo Schiavo *et. al.* [7], a coupling between the dynamics of this film layer and the acoustic mode seems required to sustain the instability. When changing the injection angle, the coherent spatio-temporal modulation of the film properties (*i.e.* height and speed) is altered (see Fig. 12 of Ref. [9]). This alteration of the film dynamics has a direct impact on the speed and the phase at which the droplets are released from the injector lip and consequently the liquid-fuel supplied to the flame root.

In the currently forced conditions, it is possible to imagine that the same behaviour appears. In the case of $\theta = 35°$, the liquid fuel droplets are injected almost directly into the combustor, penetrating deeper due to their high speed (see Fig. 11 in [9]). As a result, the liquid fuel post evaporation, mixing and burning mostly happen in the downstream flame tip region: evident from the intense heat release rate (HRR) fluctuation in that part on Fig. 5. Furthermore, the fuel burns rapidly in this region as indicated by the high-intensity heat-release perturbations being almost in-phase. Though this phase value is smaller than the expected global phase-delay, it still results in a constructive phase interference of the local flame response, thus explaining the higher global FTF gain than other injection angles.

For the other extreme case of $\theta = 60°$, the HRR fluctuations are overall moderate in strength and radially more spread-out in comparison to $\theta = 35°$. The small region of intense perturbations highlighted in Fig. 5, even though closer to the injector, yields a global FTF time-delay that is longer than for $\theta = 35°$. This also results in a better agreement with the experimentally determined value as noted in Fig. 4. However the corresponding global phase is for this case $\varphi = 0.94\pi\ rad = 170°$. In terms of local distribution, the high-intensity region and a major downstream part of flame are fluctuating around this phase value. As for the global gain, the contribution of the outer branch of the flame that is in phase opposition with the reference signal most likely contributes to the attenuation of the gain.

For the reference case of $\theta = 45°$, the FTF gain and phase values are in between that of $\theta = 35°$ and $\theta = 60°$. Similar intermediate observations apply locally, in Fig. 5. Stronger HRR fluctuation is visible in the inner branch of the flame root than in the $\theta = 35°$ case, but the local phase is here also in opposition to that of the tip regions. Overall, different parts of the high-intensity region oscillate in different phases.

5. Conclusions and Outlook

Acoustic forcing of the turbulent swirling spray flame in the SICCA-spray burner has been simulated using the Euler-Lagrange (EL) LES approach. The objective was to address such a tool's capacity to provide the Flame-Transfer-Function (FTF) and assess the suitability of the EL approach for such a system identification problem. Despite the encouraging results obtained in our previous work on *self-excited* thermoacoustic instabilities [7, 9], *forced-mode* operation is certainly showcasing difficulties. Equivalence between inlet and outlet forcing is however established numerically, although it is yet to be confirmed for other frequencies and amplitudes. Likewise, the flame response numerically retrieved still remains sensitive to general to the two-phase combustion modelling. As demonstrated, opposed trends of the FTF gain and phase are retrieved whenever investigating the sensitivity of such predictions to the prescribed spray injection angle. DMD-based local-FTF analysis complemented by a qualitative argumention based upon previous experiences for a self-sustained LES precition of the SICCA burner, provides insights as for the reasons behind the variations in global/local gain observed for the different injection angles. However, the present analysis tells little about the actual causes for such variations and what needs to be included in the two-phase flow modelling to recover experimental

measurements. Undoubtedly the observed behavior is closely linked to the liquid-film dynamics, its response to acoustics and injection angle. More rigorous quantitative analyses of the spray dynamics while submitted to acoustic forcing are therefore required to identify necessary improvements in the current modeling.

Acknowledgments

This project has received funding from the European H2020 MSCA-ITN Grant Agreement No 765998 (ANNULIGhT), the ANR16-CE22-0013 (FASMIC) and the MSCA Grant Agreement No 843958 (CLEANERFLAMES - D. L. Individual Fellowship). HPC resources from GENCI (Grant 2020-A0092B10157)) and PRACE (Grant CLEANERFLAMES 2019215145) are also acknowledged. The authors also thank S. Candel, D. Durox, A. Renaud, G. Vignat and P.R. Soundararajan from the EM2C laboratory in Paris for useful discussions and sharing of the SICCA-spray experimental data.

References

[1] S. Candel, Combustion dynamics and control: Progress and challenges, Proc. Combust. Inst. 29 (1) (2002) 1–28.

[2] T. Poinsot, Prediction and control of combustion instabilities in real engines, Proc. Combust. Inst. 36 (1) (2017) 1–28.

[3] P. Wolf, G. Staffelbach, L. Y. Gicquel, J.-D. Mueller, T. Poinsot, Acoustic and large eddy simulation studies of azimuthal modes in annular combustion chambers, Combust. Flame 159 (11) (2012) 3398–3413.

[4] A. Ghani, T. Poinsot, L. Gicquel, G. Staffelbach, LES of longitudinal and transverse self-excited combustion instabilities in a bluff-body stabilized turbulent premixed flame, Combust. Flame 162 (11) (2015) 4075–4083.

[5] A. Tyliszczak, D. E. Cavaliere, E. Mastorakos, LES/CMC of blow-off in a liquid fueled swirl burner, Flow, Turbul. Combust. 92 (1-2) (2014) 237–267.

[6] S. Tachibana, K. Saito, T. Yamamoto, M. Makida, T. Kitano, R. Kurose, Experimental and numerical investigation of thermo-acoustic instability in a liquid-fuel aero-engine combustor at elevated pressure: Validity of large-eddy simulation of spray combustion, Combust. Flame 162 (6) (2015) 2621–2637.

[7] E. Lo Schiavo, D. Laera, E. Riber, L. Gicquel, T. Poinsot, Effects of liquid fuel/wall interaction on thermoacoustic instabilities in swirling spray flames, Combust. Flame 219 (2020) 86–101.

[8] A. L. Pillai, J. Nagao, R. Awane, R. Kurose, Influences of liquid fuel atomization and flow rate fluctuations on spray combustion instabilities in a backward-facing step combustor, Combust. Flame 220 (2020) 337–356.

[9] E. Lo Schiavo, D. Laera, E. Riber, L. Gicquel, T. Poinsot, On the impact of fuel injection angle in Euler–Lagrange large eddy simulations of swirling spray flames exhibiting thermoacoustic instabilities, Combust. Flame 227 (2021) 359–370.

[10] G. Vignat, E. Lo Schiavo, D. Laera, A. Renaud, L. Gicquel, D. Durox, S. Candel, Dynamics of spray and swirling flame under acoustic oscillations : A joint experimental and LES investigation, Proc. Combust. Inst. - in press,doi:https://doi.org/10.1016/j.proci.2020.05.054.

[11] M. D. Paulhiac, B. Cuenot, E. Riber, L. Esclapez, S. Richard, Analysis of the spray flame structure in a lab-scale burner using Large Eddy Simulation and Discrete Particle Simulation., Combust. Flame 212 (2020) 25–38.

[12] M. Boileau, S. Pascaud, E. Riber, B. Cuenot, L. Y. M. Gicquel, T. Poinsot, M. Cazalens, Investigation of two-fluid methods for Large Eddy Simulation of spray combustion in Gas Turbines, Flow Turb. Combust. 80 (3) (2008) 291–321.

[13] A. Gosman, E. Loannides, Aspects of computer simulation of liquid-fueled combustors, J. Energy 7 (6) (1983) 482–490.

[14] T. Poinsot, D. Veynante, Theoretical and Numerical Combustion, 3rd Edition, 2012.

[15] F. Nicoud, L. Benoit, C. Sensiau, T. Poinsot, Acoustic modes in combustors with complex impedances and multidimensional active flames, AIAA J. 45 (2) (2007) 426–441.

[16] M. Bauerheim, F. Nicoud, T. Poinsot, Progress in analytical methods to predict and control azimuthal combustion instability modes in annular chambers, Phys. Fluids 28 (2) (2016) 021303.

[17] J. Li, D. Yang, C. Luzzato, A. S. Morgans, Open Source Combustion Instability Low Order Simulator (OSCILOS-Long) Technical report, Tech. rep., Department of Mechanical Engineering, Imperial College London, UK (2017).

[18] C. Laurent, M. Bauerheim, T. Poinsot, F. Nicoud, A novel modal expansion method for low-order modeling of thermoacoustic instabilities in complex geometries, Combust. Flame 206 (2019) 334–348.

[19] S. Candel, D. Durox, T. Schuller, J.-F. Bourgouin, J. P. Moeck, Dynamics of Swirling Flames, Annu. Rev. Fluid Mech. 46 (1) (2014) 147–173.

[20] W. Polifke, Modeling and analysis of premixed flame dynamics by means of distributed time delays, Prog. Energy Combust. Sci. 79 (2020) 100845.

[21] S. Chen, A. Lefebvre, J. Rollbuhler, Factors influencing the effective spray cone angle of pressure-swirl atomizers, J. Eng. Gas Turbines Power 114 (1) (1992) 97–103.

[22] J. Ballester, C. Dopazo, Discharge coefficient and spray angle measurements for small pressure-swirl nozzles, At. Sprays 4 (3) (1994) 351–367.

[23] G. Vignat, Dynamique de l'injection et de la combustion dans des flammes de spray swirlées et couplage azimutal dans les foyers annulaires, 2020, Université Paris-Saclay.

[24] E. J. Hopfinger, J. C. Lasheras, Explosive breakup of a liquid jet by a swirling coaxial gas jet, Phys. Fluids 8 (7) (1996) 1696–1698.

[25] M. Govindaraj, K. D. Ghate, M. S. Rao, V. S. Iyengar, S. Thirumalachari, S. Kothandaraman, Experimental study of spray breakup phenomena in small-scale simplex atomizers with and without air swirl, At. Sprays 28 (4) (2018) 299–320.

[26] K. Prieur, D. Durox, G. Vignat, T. Schuller, S. Candel, Experimental determinations of flame describing functions of swirling spray flames., in: Colloque INCA, 2017, Châteaufort, France, 2017.

[27] P. R. Soundararajan, G. Vignat, D. Durox, A. Renaud, S. Candel, Effect of Different Fuels on Combustion Instabilities in an Annular Combustor, in: ASME Turbo Expo, London, United Kingdom, 2020.

[28] K. Truffin, T. Poinsot, Comparison and extension of methods for acoustic identification of burners, Combust. Flame 142 (4) (2005) 388–400.

[29] F. Nicoud, F. Ducros, Subgrid-scale stress modelling based on the square of the velocity gradient tensor, Flow, Turbul. Combust. 62 (3) (1999) 183–200.

[30] T. J. Poinsot, S. Lele, Boundary conditions for direct simulations of compressible viscous flows, J. Comput. Phys. 101 (1) (1992) 104–129.

[31] G. Daviller, G. Oztarlik, T. Poinsot, A generalized non-reflecting inlet boundary condition for steady and forced compressible flows with injection of vortical and acoustic waves, Comput. Fluids 190 (2019) 503–513.

[32] L. Selle, F. Nicoud, T. Poinsot, Actual Impedance of Nonreflecting Boundary Conditions: Implications for Computation of Resonators, AIAA J. 42 (5) (2004) 958–964.

[33] H. Yamashita, M. Shimada, T. Takeno, A numerical study on flame stability at the transition point of jet diffusion flames, Symp. Combust. 26 (1) (1996) 27–34.

[34] B. Abramzon, W. Sirignano, Droplet vaporization model for spray combustion calculations, Int. J. Heat Mass Tran. 32 (9) (1989) 1605–1618.

[35] M. Sanjosé, J. M. Senoner, F. Jaegle, B. Cuenot, S. Moreau, T. Poinsot, Fuel injection model for Euler-Euler and Euler-Lagrange large-eddy simulations of an evaporating spray inside an aeronautical combustor, Int. J. Multiph. Flow 37 (5) (2011) 514–529.

[36] G. Chaussonnet, O. Vermorel, E. Riber, B. Cuenot, A new phenomenological model to predict drop size distribution in large-eddy simulations of airblast atomizers, Int. J. Multiph.Flow 80 (2016) 29–42.

[37] R. Gaudron, M. Gatti, C. Mirat, T. Schuller, Flame Describing Functions of a Confined Premixed Swirled Combustor With Upstream and Downstream Forcing, J. Eng. Gas Turbines Power 141 (5) (2019) 051016.

[38] P. J. Schmid, Dynamic mode decomposition of numerical and experimental data, J. Fluid Mech. 656 (2010) 5–28.